ELSEVIER

Journal of Molecular Catalysis B: Enzymatic 2 (1996) 93–101

JOURNAL OF MOLECULAR CATALYSIS B: ENZYMATIC

Kinetics of mediator-dependent pseudocatalatic activity of fungal peroxidases

J. Kulys [a,*], K. Krikstopaitis [a], S. Ebdrup [b], A. Hjelholt Pedersen [b], P. Schneider [b]

[a] *Institute of Biochemistry, Mokslininku 12, 2600 Vilnius, Lithuania*
[b] *Novo Nordisk A / S, Novo Alle, 2880 Bagsværd, Denmark*

Received 22 February 1996; accepted 18 June 1996

Abstract

The steady-state production of oxygen catalyzed by fungal *Arthromyces ramosus* peroxidase (ARP) was investigated in the pH range from 4 to 10.6. The reaction was mediated by 1-(*N*,*N*-dimethylamine)-4-(4-morpholine) benzene (AMB), 2,2′-azino-bis-(3-ethylbenzthiazoline-6-sulfonic acid) diammonium salt (ABTS) and 1,2,4,5-tetramethoxybenzene (TMB), having low (0.39 V), medium (0.7 V) and high (0.9 V) redox potentials, respectively. AMB mediated oxygen production was indicated at pH > 7, ABTS acted at pH ≥ 7 and TMB was active at pH < 7.

For evaluation of a mechanism of the pseudocatalatic reaction the mediators oxidation rate was measured at various pH. When AMB and ABTS were used the ARP activity decreased at pH > 8.5 and pK_a of transition was 9.6 and 9.5, respectively. The TMB oxidation rate reaches a maximum at pH 5.3. The rate change at pH 4–5 corresponding to a single proton transfer with pK_a 5.0 and an activity decrease at pH 5.5–7 corresponding to pK_a 5.6.

Analysis of the experimental results showed that oxygen was produced in a consecutive process including enzyme mediator oxidation and following chemical reaction of the oxidized mediator with hydrogen peroxide or its dissociated form (HO_2^-). Depending on pH the oxygen production rate was limited by the chemical or the enzymatic reaction. In the range pH 4–7 oxidized TMB reacted with hydrogen peroxide (H_2O_2), and the process was limited by the enzymatic reaction. At pH 7 and in the more alkaline area the cation radical of ABTS reacted with H_2O_2 and its dissociated form. Oxidized AMB reacted with HO_2^- at pH > 7. The oxygen production rate was correlated with the reactivity of HO_2^- estimated from the Marcus cross relationship (Marcus and Sutin, *Biochim. Biophys. Acta*, 811 (1985) 265).

Keywords: Peroxidase; *Arthromyces ramosus*; Catalase; Mediator; Hydrogen peroxide; Oxygen; *p*-Phenylenediamine; Morpholine-benzene derivatives; Azino-thiazoline-sulfonic acid derivatives; ABTS; 1,2,4,5-Tetramethoxybenzene

1. Introduction

Peroxidases play an important role in lignin degradation, synthesis of plant cell wall components and other natural and technological processes [1]. They oxidize a wide variety of organic and inorganic compounds. Oxidation of these chemicals occur via a mechanism that involves the activation of ferric peroxidases by hydrogen peroxide. Acting by mediators peroxi-

* Corresponding author.

PII S1381-1177(96)00015-X

dases can also catalyze hydrogen peroxide disproportionation (for references see [2]). For horse radish peroxidase (HRP) catalyzed reaction and in the presence of iodide it is widely accepted [2] that hypoiodous acid is generated by oxygen-atom transfer from compound I (HRP-I) which then reacts with hydrogen peroxide:

$$HIO + H_2O_2 \rightarrow O_2 + H_2O + H^+ + I^- \quad (1)$$

The two half reactions were proposed:

$$HIO + H^+ + 2e \rightarrow I^- + H_2O \quad (2)$$

$$O_2 + 2H^+ + 2e \rightarrow H_2O_2 \quad (3)$$

At pH 7 the reduction potential of the respective reactions are [3]: $E'_0 = 0.57$ V (Eq. 1) and $E'_0 = 0.30$ V (Eq. 3). At this pH the overall reaction in which hydrogen peroxide acts as reducing agent is favored by a ΔE of 0.27 V. Halide mediated catalatic activity has also been observed for thyroid- and lactoperoxidase [2]. The notable property of halogenide mediated oxygen generation is a two electron oxidation of hydrogen peroxide as described by Eq. 3.

Oxygen production from the reaction with a single oxidized mediator was indicated in a lignin peroxidase (LiP) catalyzed process [4]. Barr et al. [4] showed that oxidation of veratryl alcohol (VA) by lignin peroxidase decreased with increasing concentration of hydrogen peroxide while oxygen evolution increased. They proposed that oxygen production results from a one electron oxidation of hydrogen peroxide by the veratryl alcohol cation radical ($VA^{+\cdot}$) to yield superoxide ($O_2^{-\cdot}$), as the addition of superoxide dismutase stimulated oxygen production:

$$VA^{+\cdot} + H_2O_2 \rightarrow VA + O_2^{-\cdot} + 2H^+ \quad (4)$$

$$O_2^{-\cdot} + HO_2^{\cdot} + H^+ \rightarrow O_2 + H_2O_2 \quad (5)$$

In this work it is shown that the ability of methoxybenzenes to mediate oxygen production appeared to be related to their redox potential. However, 1,2,4,5-tetramethoxybenzene (TMB) having the lowest redox potential did not generate detectable amount of molecular oxygen. In a later paper Barr et al. [5] investigated the mechanism of peroxidase-catalyzed oxygen production by using ABTS (2,2′-azino-bis-(3-ethylbenzthiazoline-6-sulfonic acid) diammonium salt) or chlorpromazine and horseradish peroxidase or lactoperoxidase (LaP). They concluded that superoxide production catalyzed by these two peroxidases was dependent upon a compound that was oxidized by the peroxidases to a cation radical. Superoxide was subsequently produced from the one-electron oxidation of hydrogen peroxide by the cation radical.

In the single electron transfer reaction the redox potential of hydrogen peroxide oxidation is 0.94 V at pH 7.0 [3]. Due to the unfavorable thermodynamics of hydrogen peroxide oxidation with oxidized mediator (E'_0 for ABTS is 0.70 V, and E'_0 for promazine is 0.77 V [6]) a more likely reaction is an oxidation of dissociated form of hydrogen peroxide (HO_2^-). The redox potential of this reaction is $E'_0 = 0.79$ V [3]. However, HO_2^- exists only at alkaline pH as pK_a of the hydrogen peroxide dissociation is 11.62 [7]. LiP, HRP and LaP are active only in the acid, neutral or slightly alkaline area of pH, why these peroxidases are not suitable for the investigation of peroxidase pseudocatalatic activity in the alkaline range.

Fungal peroxidases, such as *Arthromyces ramosus* peroxidase (ARP) or *Coprinus cinereus* peroxidase (CiP), show activity at pH from 3 to 11 [8,9]. Therefore these enzymes are promising for investigation of the mechanism of pseudocatalatic activity over a broad range of pH. The aim of our work was to investigate the kinetics of oxygen production in ARP-catalyzed reaction. Our main attention was devoted to reactions with mediators having different redox potentials. 1-(*N*,*N*-dimethylamine)-4-(4-morpholine) benzene (AMB) was used at pH higher than 7. E'_0 of this mediator is 0.39 V [10]. ABTS having a moderate redox potential ($E'_0 =$ 0.70 V) was investigated in neutral and alkaline solutions and 1,2,4,5-tetramethoxybenzene (TMB) with $E'_0 = 0.89$ V was explored in solutions at pH below 7.

2. Experimental

2.1. Reagents used

Peroxidase from *Arthromyces ramosus* was a gift from Y. Shinmen (Suntory Ltd. Japan). The purity number (R.Z., ratio of absorbance at 405 and 280 nm) was 2.7. The concentration of ARP was determined spectrophotometrically at 405 nm using a molar absorbance of 1.04×10^5 M^{-1} cm^{-1}. AMB was synthesized by the method described in [10] and TMB was prepared as described in [11] with additional vacuum sublimation of the crystalline product.

Solutions of hydrogen peroxide were prepared from perhydrol (30%) and the concentrations were determined using the molar absorbance at 240 nm ($\varepsilon_{240} = 39.4$ M^{-1} cm^{-1}). All solutions of enzyme and hydrogen peroxide were prepared on the basis of double-distilled water. AMB was dissolved in ethanol, ABTS and TMB were dissolved in buffer solution.

2.2. Kinetic and electrochemical measurements

The pseudocatalatic reaction was investigated in a 10.0 ml glass cell thermostated at 25 or 30°C. Kinetics of the reaction was followed by the oxygen concentration increase measured with an membrane-type oxygen sensitive electrode using a computer-controlled system. Measurements were performed in 0.1 M sodium acetate, 0.05 M sodium phosphate, in the mixture of 33 mM disodium phosphate, 33 mM boric acid, 33 mM sodium carbonate buffer and in 0.05 M disodium carbonate. The pH of the buffer solutions was adjusted with 3 M hydrochloric acid or 3 M sodium hydroxide solution. In the case of AMB the reaction mixture contained 0.25 mM AMB, 10–120 nM ARP, 0.1–1.6 mM H_2O_2. The final concentration of ethanol in the AMB solution was 1% (v/v). The process was evaluated at 25°C. In the case of ABTS the reaction was performed in a buffer solution containing 7.6 nM of ARP, 1.06 mM of ABTS and 1.08 mM of hydrogen peroxide at 30°C. The TMB reaction mixture contained 12.2 nM of ARP, 0.96 mM of TMB and 1.08 mM of hydrogen peroxide, the reaction was evaluated at 30°C and initiated by adding hydrogen peroxide with a Hamilton syringe following a 10 s delay after system launch. The kinetics of O_2 generation was measured during 3 min. For calculations the concentration of oxygen in the buffer solutions was assumed to be 0.253 and 0.232 mM at 25 and 30°C, respectively [3].

Kinetics of mediators oxidation was performed by using spectrophotometric method. Kinetic curves and absorption spectra were registered by spectrophotometer Beckman DU-8B. The generation of single oxidized forms were measured at 604 nm (AMB), 414 nm (ABTS) and 450 nm (TMB). The kinetics of AMB and ABTS oxidation was performed at pH 6.0–10.8, by using the buffer system containing 33 mM disodium phosphate, 33 mM boric acid and 33 mM sodium carbonate. The concentration of substrates, ARP and hydrogen peroxide was 0.1 mM, 2 nM and 0.1 mM, respectively. Kinetics of the TMB oxidation was evaluated at pH 4–7 in 0.05 M sodium phosphate. The concentration of the TMB, ARP and the hydrogen peroxide was 0.9 mM, 6.1 nM and 0.1 mM. The extinction coefficients of the corresponding oxidized substrates AMB and ABTS were 9.8×10^3 M^{-1} cm^{-1} and 3.6×10^4 M^{-1} cm^{-1} [10]. The extinction coefficient of TMB (8.9×10^3 M^{-1} cm^{-1}) was determined by titration of 0.1 mM TMB solution with hexachloroiridate in 0.05 M phosphate buffer solution at pH 7.0.

Kinetics of AMB cation radical ($AMB^{+\cdot}$) oxidation was measured at 604 nm in the 0.05 M phosphate buffer pH 7.0 at 25°C. The $AMB^{+\cdot}$ was accumulated by the using 2 nM of ARP and 50 μM of H_2O_2. The concentration of AMB was varied from 0.05 to 0.25 mM. The oxidation of $AMB^{+\cdot}$ following solution bleaching was initiated by adding 100 nM of ARP and 50 μM of H_2O_2.

Protonation of AMB was measured by spectrophotometrical titration in 0.05 mM acetate and 0.05 mM phosphate buffer solutions. The absorbance change was measured at 295 nm.

The formal redox potentials of ABTS and TMB were determined by cyclic voltammetry using a glassy carbon electrode and a potential scan rate of 100 mV/s. For measurements an electroanalytical system (Cypress Systems, Inc., USA) and a glassy carbon electrode (model CS-1087, Cypress Systems, Inc., USA) were used. The reference electrode used was a saturated calomel electrode (SCE saturated with KCl, mod. K-401, Radiometer, Denmark) and the auxiliary electrode used was a Pt-wire (diameter 0.2 mm, length 4 cm) mounted at the end of the reference electrode. The redox potential was calculated using the formula $(E_a + E_c)/2$, where E_a and E_c are the potentials of the anodic and cathodic peaks, respectively. The concentration of the compounds were 2 mM. The potential of ABTS was determined in 50 mM phosphate buffer pH 7.0 containing 0.1 M sodium chloride. The potential of TMB was measured in 0.1 M sodium acetate pH 4.0–6.0 with increments of 0.5 pH unit. The calculated redox potential of ABTS was 456.1 ± 3.7 mV (at pH 7.0) and for TMB it was 647.2 ± 1.9 mV (at pH 4–6) vs. SCE (700 and 891 mV vs. SHE, respectively). Double potential step chronoamperometric measurements of AMB were performed in 0.05 M sodium phosphate (pH 7.0) and 0.05 M carbonate buffer solutions (pH 10) containing 0.1 M sodium chloride and 1% (v/v) of ethanol. For the measurements, the glassy carbon, reference and auxiliary electrodes were used as described above. Duration time of potential step was 0.1 s, forward potential changed from 0 to 0.3 V and reverse potential changed from 0.3 to 0 V.

2.3. Calculations

Kinetic data were transferred to Mathcad 3.1 Windows version which was used for calculations and plots below. The kinetic curves of the time dependent on oxygen concentration were extrapolated with the third order polynomial. The approximation of data was performed by minimizing the mean squared error (MSE). Estimation of the kinetic constant of cation radical of AMB decomposition and its half-life was performed as described in [12].

3. Results and discussion

3.1. The rate of oxygen production and mediator oxidation

The ARP-catalyzed production of oxygen is mediator dependent. When AMB was used as mediator the oxygen production rate was largest at pH 9–10. Kinetic curves of ARP-catalyzed oxygen generation show *S*-shape type (Fig. 1). Oxygen production reaches steady-state level after a time which depends on concentration of H_2O_2. It was reached after 50 s at 0.1 mM of hydrogen peroxide and after 150 s at 1.6 mM of H_2O_2. The amount of oxygen produced varied from 9 to 28% of the amount of hydrogen peroxide on a molar basis. This indicates that the yield of molecular oxygen produced in the catalatic process (Eq. 6) was 18–56%:

$$2H_2O_2 \rightarrow O_2 + 2H_2O \quad (6)$$

The appearance of lag time in the kinetic curves of oxygen production indicates that oxygen is generated in a consecutive process. The steady-state level of oxygen production can be

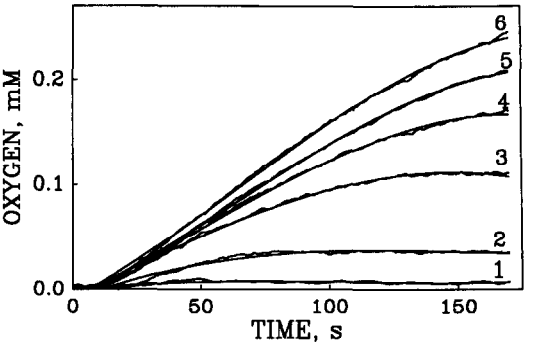

Fig. 1. Dependence of oxygen formation rate on hydrogen peroxide concentration. The reaction mixture contained 0.25 mM AMB, 30 nM ARP, 0.1 (1), 0.2 (2), 0.4 (3), 0.6 (4), 1.0 (5), 1.6 mM (6) of H_2O_2 in 0.05 M carbonate buffer (pH 10.0), 25°C. RE of the polynomial approximations was 3.0 (1), 3.5 (2), 2.5 (3), 2.4 (4), 1.9 (5) and 1.5 (6) %.

due to various factors, among them hydrogen peroxide consumption, decomposition of oxidized mediator and enzyme inactivation. The amount of oxygen produced, however, indicates that the amount of hydrogen peroxide is not a limiting factor. Since saturation of the reaction rate was indicated at various pH it cannot be explained by enzyme inactivation or mediator decomposition. Direct measurements of half-life of oxidized AMB performed by a chronoamperometric method indicates that even at pH 10 it was more than 4 s. The most probable reason of the steady-state level of oxygen production is an oversaturation by oxygen in the buffer solution and its release into micro bubbles in the cell. To overcome the complicated character of the kinetic curves, oxygen production was approximated by a third order polynomial (Fig. 1). The relative error (RE) of approximation, expressed (in percent) as the ratio of $\sqrt{MSE}$ and the mean value, changed from 1.5 to 3.5%. The oxygen production rate calculated as maximum differential of the polynomial approximation was established at 20–40 s, and it depends on the hydrogen peroxide concentration. At this time the concentration of oxygen produced exceeded the atmospheric saturated concentration by less than 30% (Fig. 1).

At pH 10 the dependence of oxygen production rate on hydrogen peroxide concentration

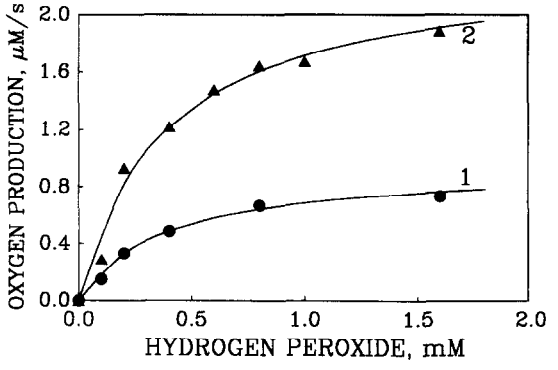

Fig. 2. Dependence of oxygen production rate on hydrogen peroxide concentration. 0.05 M carbonate buffer, pH 10.0, 25°C, 0.25 mM AMB, 10 nM ARP (1), 30 nM ARP (2). RE of the polynomial approximations were 2.2–3.5% (1) and 1.5–3.5% (2).

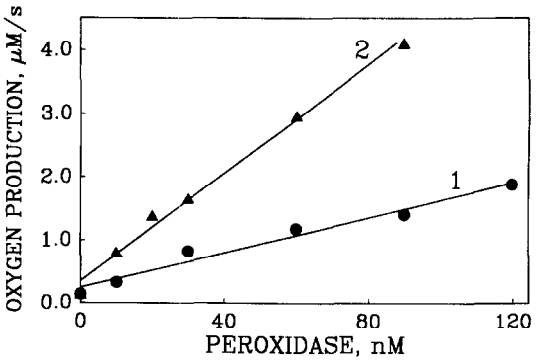

Fig. 3. Dependence of oxygen production on ARP concentration. 0.2 (1), 1.0 mM (2) H_2O_2, other experimental conditions as in Fig. 2. RE of polynomial approximations were 1.4–4.7% (1) and 0.95–4.5% (2).

shows a typical hyperbolic saturation shape (Fig. 2). Maximum rates (V_m) and apparent Michaelis constants ($K_{M(app)}$) were calculated according to the Michaelis–Menten equation. At ARP concentrations of 10 nM and 30 nM, $K_{M(app)}$ was the same 0.38 ± 0.07 mM, and V_m was 0.95 ± 0.07 μM/s and 2.37 ± 0.18 μM/s, respectively. Different V_m values indicate that the process depends on the enzyme activity. The limitation of the process by the enzymatic reaction is confirmed by measurements of oxygen production rate dependence on ARP concentration (Fig. 3). At two hydrogen peroxide concentrations (0.2 and 1 mM) oxygen production rate linearly depends on ARP concentration up to 120 nM.

The pH dependence of the ARP-catalyzed pseudocatalatic process in the range from pH 7.0 to 10.5 is shown in Fig. 4. Oxygen production rate was normalized to the enzyme concentration and was multiplied by a factor of two. The maximal rate is obtained at pH about 9.4. The reaction rate drops fast in more alkaline and acidic solutions, and at pH 7.0 the reaction rate is negligible.

For evaluation of the pseudocatalatic reaction mechanism the dependence of AMB oxidation catalyzed by ARP was measured at pH 6.1–10.8 (Fig. 4). Experimental results show that the ARP activity decreases at pH > 8.5. This activ-

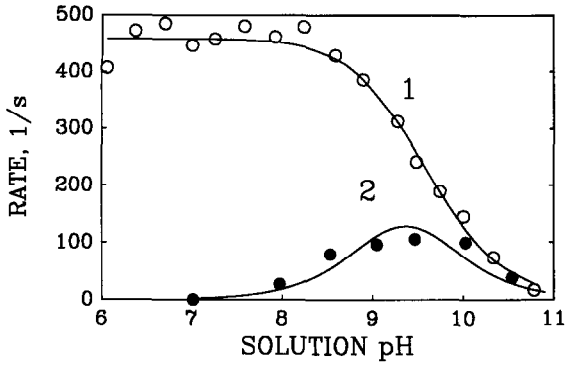

Fig. 4. Dependence of AMB oxidation (1) and AMB-mediated oxygen production rate (2) on solution pH at 25°C. Circles correspond to experimental data, solid curves represent calculated values. The buffer system used: 33 mM disodium phosphate, 33 mM boric acid, 33 mM sodium carbonate. ARP 2 nM (1) and 30 nM (2), H_2O_2 0.1 mM (1) and 1.0 mM (2), AMB 0.1 mM (1) and 0.25 mM (2).

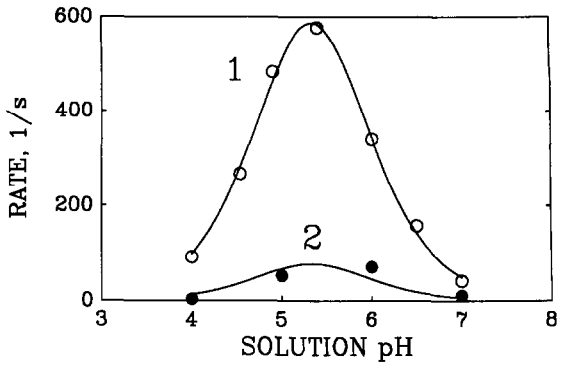

Fig. 6. Dependence of TMB oxidation (1) and TMB-mediated oxygen production rate (2) on solution pH at 30°C. Circles correspond to experimental data, solid curves represent calculated values. The buffer system used 0.05 M sodium phosphate, ARP 6.1 nM (1) and 12.2 nM (2), H_2O_2 0.1 mM (1) and 1.1 mM (2), TMB 0.9 mM (1) and 1.0 mM (2).

ity change is related to single proton transfer, as can be described by the equilibrium:

$$ARP^{N-} \rightleftharpoons ARP^{(N+1)-} + H^+ \quad (7)$$

where $ARP^{(N+1)-}$ represents completely inactive ARP, and N corresponds to protein charge at $pH = pK_a$.

The pK_a of this transition was 9.59 (RE of approximation was 6.3%). At pH 7.0 the oxidation rate normalized to enzyme concentration was 458 s^{-1}.

ABTS mediated oxygen production was measured at pH 7–10.2 (Fig. 5). In contrast to the AMB mediated oxygen production, ABTS is efficient even at pH 7.0. As with AMB, the rate decreases at pH higher than 9.5.

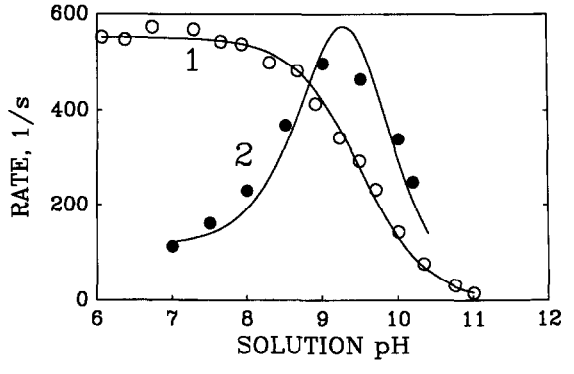

Fig. 5. Dependence of ABTS oxidation (1) and ABTS-mediated oxygen production rate (2) on solution pH at 30°C. Circles correspond to experimental data, solid curves represent calculated values. The buffer system used: 33 mM disodium phosphate, 33 mM boric acid, 33 mM sodium carbonate. ARP 2 nM (1) and 7.6 nM (2), H_2O_2 0.1 mM (1) and 1.1 mM (2), ABTS 0.1 mM (1) and 1.1 mM (2).

The ABTS oxidation rate also depends on pH and it drops at pH higher than 8.0 (Fig. 5). The decrease of oxidation rate is consistent with a single proton transfer (Eq. 7). An apparent pK_a of transition was very similar to AMB (9.50; RE of approximation was 4.3%).

The TMB mediated oxygen production dependence on pH shows a quite different shape in comparison to AMB and ABTS (Fig. 6). In the case of the TMB maximal oxygen generation rate is obtained at pH 5.5 and it decreases in more acid or alkaline area. Oxygen production rate also depends on buffer components. At pH 6.0 and in 0.1 M acetate buffer solution it was 2.4 times higher in comparison to 0.05 M phosphate buffer. In phosphate buffer solution the oxygen production rate correlates with TMB oxidation over the whole pH range tested (Fig. 6). The increase of TMB oxidation rate at pH 4–5 corresponds to a single proton transfer with pK_a 5.03 ± 0.07. Decrease of activity at pH 5.5–7 corresponds also to single proton transfer and pK_a of this transition was determined to 5.64 ± 0.07. In the whole pH interval ARP activity changes can be illustrated by the follow-

ing scheme (Eq. 8) in which only the $ARP^{(n-1)+}$ form is active with TMB:

$$ARP^{n-} \rightleftharpoons ARP^{(n+1)-} + H^+ \rightleftharpoons ARP^{(n+2)-} + H^+ \quad (8)$$

where n corresponds to the protein charge at pH 5.03 ($n < N$ from Eq. 7).

Similar values of pK_a for two non-phenolic substrates (AMB and ABTS) indicate that the activity of ARP in alkaline solution is determined by deprotonation of the same group of enzyme molecule. The crystal structure of ARP was derived very recently [13]. Three basic amino acid residues, Arg48, Lys49 and Arg52, interact by hydrogen bonds with the propionate groups of the heme via water molecules. Single proton transfer in this concert may control the AMB and ABTS oxidation rate. The protonation of the same propionate group at pH 5 can be responsible for TMB activity decrease in the acid area of pH. The pK_a value 5.64 is close to that for histidine protonation. Distal His56 in ARP is bound to heme by a hydrogen bond via a water molecule. The role of this distal histidine has been discussed in many publications. Bhattacharyya et al. [14] claimed that in HRP the distal histidine controls the aromatic donor oxidation by regulation of electron transport without effecting the donor binding or compound **I** formation. This detailed investigation has shown that deprotonation of histidine in compound **I** and compound **II** can be responsible for the activity change at pH 6. It is possible that deprotonation in the ARP molecule of this distal histidine controls the TMB oxidation rate, too. The activity dependence on pH indicates that non-phenolic substrates like AMB and ABTS interact with the same ARP residues, whereas TMB interacts with some other residues of the enzyme molecule.

3.2. Kinetic scheme of the ARP-catalyzed pseudocatalatic process

The oxygen production in a mediator-dependent peroxidase reaction is a result of the consecutive enzymatic and chemical process with the corresponding rates V_{enz} and V_{chem}. The steady state rate of oxygen production (V_0) can be derived:

$$V_0 = \frac{V_{enz} V_{chem}}{V_{enz} + V_{chem}} \quad (9)$$

In the case of the low redox potential mediator (AMB) the rate of oxygen production at pH 7.0 is very low (Fig. 4). However, the enzyme-catalyzed mediator oxidation at this pH is high. So that the overall process is limited by the chemical reaction and $V_0 = V_{chem}$. At higher pH the chemical process is fast and the overall process is limited by the enzymatic reaction ($V_0 = V_{enz}$). Strong support for process limitation by enzymatic reaction comes from the dependence of the oxygen production rates on the amount of enzyme (Fig. 3). When the pH changes from 7 to 10, while the chemical reaction rate increases significantly the enzymatic activity decreased about 3 times (Fig. 4, curve 1), the limiting step changes. This is caused by dissociation of hydrogen peroxide and reduction of the oxidized mediator by HO_2^- (Eq. 10):

$$M^{+\cdot} + HO_2^- \rightarrow M + O_2^{-\cdot} + H^+ \quad (10)$$

Most probably the oxygen at high pH is generated in a thermodynamically favorable secondary reaction of superoxide with another oxidized mediator molecule:

$$M^{+\cdot} + O_2^{-\cdot} \rightarrow M + O_2 \quad (11)$$

In the whole pH range, the rate of oxygen production is a result of the changes in the enzymatic activity and chemical reaction rate. The calculated overall process is represented by curve 2 in Fig. 4.

In alkaline solutions the ABTS mediated process is similar to AMB (Fig. 5). However, in the ABTS mediated process oxygen is produced even at pH 7. This indicates that cation radicals of ABTS react with both undissociated and dissociated hydrogen peroxide. The reaction of hydrogen peroxide is possible due to the high redox potential of the mediator.

The TMB has a higher redox potential than ABTS. This is the reason why protonated superoxide is generated (Eq. 12) in TMB mediated process even in acid solutions and a fast disproportionation of superoxide generates oxygen.

$$TMB^{+\cdot} + H_2O_2 \rightarrow TMB + HO_2^{\cdot} + H^+ \quad (12)$$

However, the simultaneous change of peroxidase-catalyzed TMB oxidation rate and oxygen production at various pH (Fig. 5) indicates that the process is limited by the enzyme reaction. A comparison of the normalized activity and the pseudocatalatic activity rates shows that only a portion (about 25% if the stoichiometry of reaction is 2 moles of cation–radical and 1 mole of oxygen) of the oxidized mediator produces oxygen. This can be caused by a parallel nucleophilic reaction of oxidized mediator with water. The low enzymatic TMB oxidation rate by LiP and a parallel TMB cation radical conversion may be the reason why oxygen production was not detected in [4].

3.3. Calculation of reactivity of hydrogen peroxide species

The results of oxygen production in alkaline solutions permit to calculate the rate of cation–radical interaction with hydrogen peroxide species. As mentioned above ABTS- and AMB-mediated processes are limited by the chemical reactions at pH 8.5 (Figs. 4 and 5). For this reason an apparent bimolecular constant of oxidation of dissociated hydrogen peroxide by oxidized mediator (M) can be expressed as a second order reaction:

$$d[O_2]/dt = k_{(app)}[M^{+\cdot}][HO_2^-] \quad (13)$$

As the process is limited by the chemical reaction, the steady-state $M^{+\cdot}$ concentration is very close to the total concentration of M, and the amount of HO_2^- can be derived from pK_a of hydrogen peroxide (11.62 [7]). For ABTS the calculated $k_{(app)}$ is 3.2×10^3 M^{-1} s^{-1} and for AMB it is 1.1×10^4 M^{-1} s^{-1}. Assuming that the interaction of mediators with hydrogen peroxide species occurs similarly to the autooxidation of other closed-shell organics [15], the rate of reaction (Eq. 13) can be calculated by using the Marcus cross relationship [16]. Reorganization energy for the reaction (Eq. 14) can be derived (Eq. 15):

$$HO_2^{\cdot} + M \rightleftharpoons HO_2^- + M^{+\cdot} \quad (14)$$

$$\lambda = 4RT\ln(Z) - 2RT\ln(k_{11}k_{22}) \quad (15)$$

where Z was set to 10^{11} M^{-1} s^{-1} [15], k_{11} is a self-exchange constant for the $HO_2^{\cdot}/HO_2^-$ couple and k_{22} is a self-exchange constant for the $M^{+\cdot}/M$ couple. $k_{11} = 17$ M^{-1} s^{-1} was calculated in [17] and k_{22} here was assumed to be 10^8 M^{-1} s^{-1} as for other organics [15].

The expression for the rate of direct reaction (Eq. 14) (k_{12}) is:

$$\ln(k_{12}) = \ln(Z) - \lambda/4RT\left(1 - RT/\lambda\ln(K_{12})\right)^2 \quad (16)$$

where the equilibrium constant K_{12} can be calculated from the redox potential of $HO_2^{\cdot}/HO_2^-$ and $M^{+\cdot}/M$ couples.

At pH 8.5, assuming a redox potential of 0.79 V for HO_2^- [3], gives k_{-12} values ($k_{-12} = k_{12}/K_{12}$) of 6.2×10^3 $M^{-1}s^{-1}$ and 6.2 $M^{-1}s^{-1}$ for ABTS and AMB, respectively. The value for ABTS is similar that determined experimentally. However, for AMB the calculations give a much lower constant. One explanation of the experimentally determined high AMB reactivity can be that electron transfer is coupled to proton transfer [18]. At pH 8.5 the redox potential of the proton coupled oxidation of HO_2^- decreases up to 0.57 V [3]. The two unprotonated *n*-electron orbitals of the nitrogen atoms (pK_a of AMB protonation is 5.7 ± 0.1) may support coupled proton transfer. The potential value will give $k_{-12} = 0.9 \times 10^3$ M^{-1} s^{-1} which is still lower than that determined experimentally. Another explanation for the high AMB reactivity can be related to an additional oxidation of $AMB^{+\cdot}$. The apparent bimolecular constant of $AMB^{+\cdot}$ oxidation is 85 times less than that of AMB, but the rather high stability of $AMB^{+\cdot}$

(half-life is more than 4 s) may favor this reaction. The redox potential of couple $AMB^{2+}/AMB^{+\cdot}$ is established to be 0.71 V vs. SHE and for this reason the AMB^{2+} interaction with HO_2^- is thermodynamically favored.

Acknowledgements

We are grateful to Y. Shinmen for the gift of *Arthromyces ramosus* peroxidase. Financial support of K. Krikstopaitis as a post-graduate student at the Vytautas Magnus University (Kaunas, Lithuania) is acknowledged.

References

[1] K.E.L. Eriksson, R.A. Blanchette and P. Ander, Microbial and Enzymatic degradation of Wood and Wood Components, Springer-Verlag, Berlin, Heidelberg, 1990, p. 225–334.
[2] H.B. Dunford, Horseradish Peroxidase: Structure and Kinetic Properties, in J. Everse and K. Everse (Eds.), Peroxidases in Chemistry and Biology, Vol. 2, CRC Press, Boca Raton, FL, Ann Arbor, MI, Boston, MA, 1991, p. 1–25.
[3] W.H. Koppenol, Adv. Free Radical Biol. Med., 1 (1985) 91.
[4] D.P. Barr, M.M. Shah and S.D. Aust, J. Biol. Chem., 268 (1993) 241.
[5] D.P. Barr and S.D. Aust, Arch. Biochem. Biophys., 303 (1993) 377.
[6] C. Bourdillon, C. Demaille, J. Moiroux and J.-M. Saveant, J. Am. Chem. Soc., 115 (1993) 2.
[7] Handbook of Chemistry and Physics, 74th Ed., CRC Press, Boca Raton, FL, p. 8–47.
[8] Y. Shinmen, S. Asami, T. Amachi, S. Shimizu and H. Yamada, Agric. Biol. Chem., 50 (1986) 247.
[9] M. Kjalke, M.B. Andersen, P. Schneider, B. Christensen, M. Schülein and K.G. Welinder, Biochim. Biophys. Acta, 1120 (1992) 248.
[10] J. Kulys, T. Buch-Rasmussen, K. Bechgaard, V. Razumas, J. Kazlauskaite, J. Marcinkeviciene, J.B. Christensen and H.E. Hansen, J. Mol. Catal., 91 (1994) 407.
[11] A. Zweig, W.G. Hodgson and W.H. Jura, J. Am. Chem. Soc., 86 (1964) 4124.
[12] A.J. Bard and L.R. Faulkner, Electrochemical Methods. Fundamentals and Applications, John Wiley and Sons, New York, 1980, p. 451.
[13] N. Kunishima, K. Fukuyama, H. Matsubara, H. Hatanaka, Y. Shibano and T. Amachi, J. Mol. Biol., 235 (1994) 331.
[14] D.Kr. Bhattacharyya, U. Bandyopadhyay and R.K. Banerjee, J. Biol. Chem., 268 (1993) 2292.
[15] G. Merenyi, J. Lind and M. Jonsson, J. Am. Chem. Soc., 115 (1993) 4945
[16] R. Marcus and N. Sutin, Biochim. Biophys. Acta, 811 (1985) 265
[17] J. Lind, X. Shen, G. Merenyi and B.-O. Jonsoon, J. Am. Chem. Soc., 111 (1989) 7654.
[18] R.A. Binstead, M.E. McGuire, A. Dovletoglou, W.K. Seok, L.E. Roecker and T.J. Meyer, J. Am. Chem. Soc., 114 (1992) 173.